

Analysis of photonic band structure of 2-D metallic-dielectric photonic crystals suitable for various applications in optical communications

M. Masoudi^{1,*}, G. Darvish², E. Darabi¹

¹Plasma physics research center, Science and Research Branch, Islamic Azad University, Tehran, Iran.

²Electrical Engineering Department, Science and Research Branch, Islamic Azad University, Tehran, Iran.

Received: 2 June 2011/Accepted: 10 August 2011/ Published: 20 September 2011

Abstract

We numerically analyzed the photonic band structure of 2-D metallic-dielectric photonic crystal structures which consist of square arrays with circular metal rods. We calculated dispersion curves of square lattice with metal rods which are embedded into background materials with different dielectric constants for TM and TE modes and changed the ratio of the rods' radius to the lattice constant (r/a). We also investigated the effect of changing metal rods on the photonic band structures in two steps. In the first step, we changed background materials with fixed r/a constant and then we fixed both the r/a ratio and background dielectric constants. Because we designed our structure in a way that the photonic band gaps appear in a range of telecommunication wavelength the results showed that these structures will be applicable in different photonic devices such as optical filters.

PACs: 42.70.Qs; 02.70.Bf; 42.79.Sz; 64.70.kd

Keywords: *Metallic Dielectric Photonic Crystal; Square lattice; metal rod; Finite Difference Time Domain method; Drude model*

1. Introduction

In recent years lots of attention have gone to study photonic crystals especially metallic-dielectric photonic crystals because of their application in optical communication systems. Photonic crystals (PhCs) are inhomogeneous dielectric media with periodic refractive index and they have a photonic band gap in general. The photonic band gap is the range of frequencies in which light cannot propagate through the structure. If instead of dielectric inclusion we put metals in dielectric background we will have metallic-dielectric photonic crystal (MDPC) which has more interesting properties than PhCs [1-5] which we will study some of them in this work. In comparable with PhCs, MDPCs have cutoff frequency for TM modes, and their widths of their gaps are wider than PhCs, but more interesting properties of these structures is that because of these properties their size will be more smaller than similar typical PhCs [6,7]. Most researches have done in microwave ranges [8, 10] but by suitable design of PBG structures we tried to get photonic band gaps in a range of telecommunication wavelength. Hence these structures will be applicable in different photonic devices such as optical filters, polarizer, or waveguide, and optical modulators [9-12]. For achieving this goal we used metallic scatterers, instead of dielectric, in dielectric background. We

saw by careful designing metallic photonic crystals that we can obtain wide photonic band gaps in comparable with PhCs. In this work, we calculate the dispersion curves for square lattice of circular metal rods embedded into backgrounds with different dielectric constants for normal incident wave by means of softwares which are in accordance with finite-difference time-domain method and the dielectric constant of rods modeled by Drude dispersion relation. Organization of this paper is as follows: in Section 2, we present the theoretical background and the method of Analysis. Section 3 covers the simulation results obtained for the MPDC structures. We show the photonic band gaps for different specifications of MPDCs. Finally, we conclude this paper in Section 4.

2. Theoretical background

A) We consider metal an isotropic medium with dielectric constant ϵ , permeability μ , and conductivity σ . By using the material equations for electric displacement field D , magnetic flux density B , current density J , and charge density ρ , Maxwell's equations can be written as [13,14]:

$$\begin{aligned} \vec{D} &= \epsilon \vec{E}, & \vec{B} &= \mu \vec{H}, & \vec{J} &= \sigma \vec{E} + (J_0 = 0) \\ \nabla \times \vec{E} + \mu \frac{\partial \vec{H}}{\partial t} &= 0 \end{aligned} \quad (1)$$

We assume a monochromatic plane wave description for the electric and magnetic fields:

*Corresponding author: M. Masoudi;
E-mail: m.masoudi@srbiau.ac.ir
Tel: (+98) 09124941487
Fax: (+98) 021 44470511

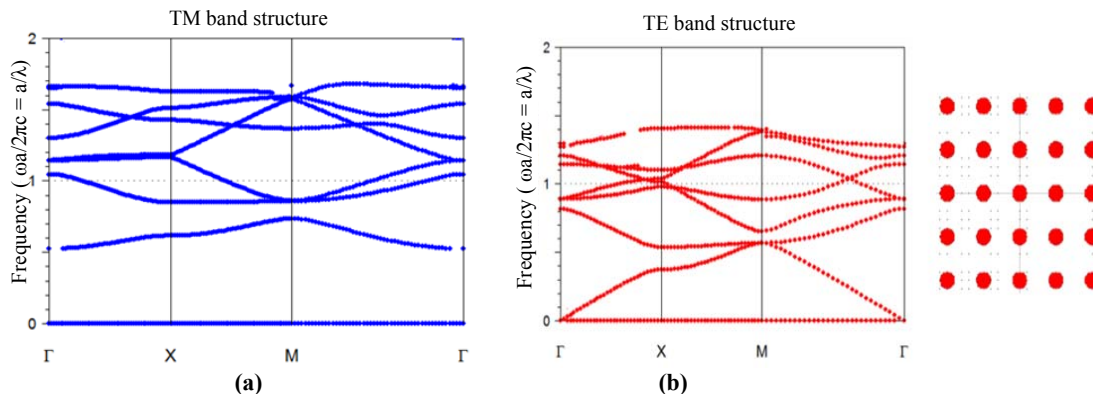


Fig. 1. Photonic band diagrams for square lattice with copper rods in air background ($r/a=0.2$). The first 8 bands for TM (a) and TE (b) modes.

$$\nabla \times \vec{H} - \epsilon \frac{\partial \vec{E}}{\partial t} = \sigma \vec{E} \tag{2}$$

$$\vec{E} = \vec{E}_0 e^{-i\omega t}, \quad \vec{H} = \vec{H}_0 e^{-i\omega t} \tag{3}$$

Hence, wave equation for a metal can be written as:

$$\nabla^2 \vec{E} + \hat{K}^2 \vec{E} = 0 \tag{4}$$

$$\hat{K}^2 = \omega^2 \mu \left(\epsilon + i \frac{\sigma}{\omega} \right) \tag{5}$$

where \hat{K} is complex dielectric constant, defined by:

$$\hat{K} = K + i \frac{\sigma(\omega)}{\epsilon_0 \omega} = K_r + iK_i, \quad \sigma(\omega) = \frac{\sigma_0}{1 - i\omega\Gamma} \tag{6}$$

where $\sigma(\omega)$ is ac conductivity, σ_0 is the conductivity measured with DC electric field, and Γ is the damping constant. The dielectric constant of a medium is dependent on how the charges within the material respond to an optical field.

B) According to Drude model, the motion equation of an electron (with m and e the mass and the charge respectively) with velocity v in a material can be written as:

Table 1. Bandgaps for Copper rods in square lattice with different r/a ratio, center wavelength: $1.55\mu\text{m}$ ($n_{\text{cu}}=0.606+i8.26$), and air background.

TE mode		TM mode	
r/a	$\frac{\omega a}{2\pi c} = \frac{a}{\lambda}$	r/a	$\frac{\omega a}{2\pi c} = \frac{a}{\lambda}$
0.05	-	0.05	(TM0-1)=0.290
0.1	-	0.1	(TM0-1)=0.353
0.2	-	0.2	(TM0-1)=0.5 (TM1-2)=0.09
0.28	-	0.3	(TM0-1)=0.7469 (TM1-2)=0.257
0.3	(TE1-2)=0.027 (TE3-4)=0.017	0.32	(TM0-1)=0.7959 (TM1-2)=0.2973
0.32	(TE1-2)=0.018 (TE3-4)=0.009	0.4	(TM0-1)=1.04 (TM1-2)=0.52 (TM3-4)=0.14
0.4	(TE1-2)=0.113		

ten as:

$$m \frac{d\vec{v}}{dt} + m\vec{v}\Gamma = -e\vec{E} \tag{7}$$

Table 2. Bandgaps for noble metal rods in square lattice with $r/a = 0.2$ ratio, center wavelength: $1.55\mu\text{m}$, with different backgrounds.

$r/a = 0.2$			
Background	Rod	$\frac{\omega a}{2\pi c} = \frac{a}{\lambda}$	
		TE mode	TM mode
air	Ag	-	(TM0-1)=0.529 (TM1-2)=0.116
air	Au	-	(TM0-1)=0.532 (TM1-2)=0.12
air	Cu	-	(TM0-1)=0.5 (TM1-2)=0.09
InP	Ag	-	(TM0-1)=0.15 (TM1-2)=0.0337
InP	Au	-	(TM0-1)=0.15 (TM1-2)=0.034
InP	Cu	-	(TM0-1)=0.149 (TM1-2)=0.032

In the harmonic regime, equation (7) and Maxwell equations lead to the following relations:

$$\vec{j}(\omega) = \sigma(\omega)\vec{E} = \frac{Ne^2}{m(\Gamma - i\omega)} \vec{E}_0 = \frac{Ne^2}{m(\Gamma - i\omega)} \vec{E}_0 \tag{8}$$

$$\epsilon(\omega) = \epsilon_\infty - \frac{\omega_p^2}{\omega(\omega + i\Gamma)}, \quad \omega_p^2 = \frac{Ne^2}{m\epsilon_0} \tag{9}$$

$$\epsilon_r(\omega) = \epsilon_\infty - \frac{\omega_p^2}{(\omega^2 + \Gamma^2)}, \quad \epsilon_i(\omega) = \frac{\omega_p^2 \Gamma}{\omega(\omega^2 + \Gamma^2)} \tag{10}$$

3. Simulation results

A. Our goal in this section is to calculate the photonic band structures of the 2-D square lattice of circular copper rods which are embedded into air

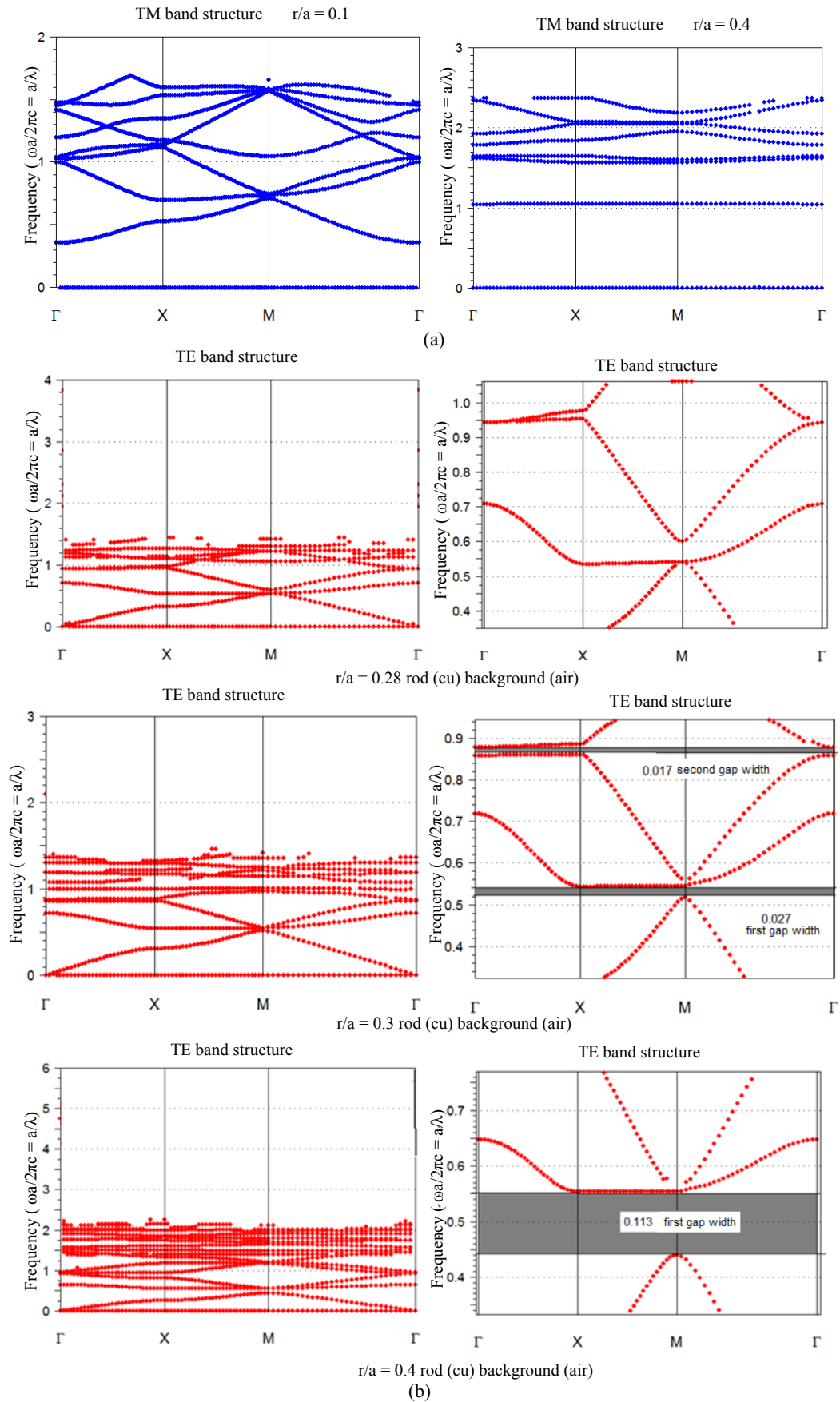


Fig. 2. Photonic band diagrams for square lattice with copper rods in air background for different r/a ratio for TM (a) and TE (b) modes.

Table 3. Bandgaps for Copper rods in square lattice with different $r/a(0.2,0.4)$ ratio, center wavelength: $1.55\mu\text{m}$ ($n_{\text{Cu}}=0.606+i8.26$), with different backgrounds.

$r/a=0.2$		$r/a=0.4$		
Background	TM mode $\frac{\omega a}{2\pi c} = \frac{a}{\lambda}$	Background	TM mode $\frac{\omega a}{2\pi c} = \frac{a}{\lambda}$	TE mode $\frac{\omega a}{2\pi c} = \frac{a}{\lambda}$
Air	(TM0-1)=0.5 (TM1-2)=0.09	Air	(TM0-1)=1.04 (TM1-2)=0.52 (TM3-4)=0.14	(TE1-2)=0.11
CdS	(TM0-1)=0.224 (TM1-2)=0.05	Alumina	(TM0-1)=0.35 (TM1-2)=0.17	(TE1-2)=0.037
Alumina	(TM0-1)=0.174 (TM1-2)=0.039	Si	(TM0-1)=0.3 (TM1-2)=0.15	(TE1-2)=0.033
Si	(TM0-1)=0.151 (TM1-2)=0.033	InP	(TM0-1)=0.29 (TM1-2)=0.143	(TE1-2)=0.032
InP	(TM0-1)=0.149 (TM1-2)=0.032	GaAs	(TM0-1)=0.28 (TM1-2)=0.14	(TE1-2)=0.031
GaAs	(TM0-1)=0.144 (TM1-2)=0.03	Ge	(TM0-1)=0.26 (TM1-2)=0.13	(TE1-2)=0.028
Ge	(TM0-1)=0.130 (TM1-2)=0.029			
PbTe	(TM0-1)=0.094 (TM1-2)=0.021			

background, with different values of the rods radius/lattice constant ratio (r/a) for TM and TE modes. The simulation results are shown in Figs. 1 and 2. As illustrated in Fig. 1, a cutoff frequency exists for TM modes even for very small r/a ratios. Details of our simulation results are summarized in Table. 1. As is noticeable from Table. 1, TM modes have a cutoff frequency and their bandgaps appear as soon as r/a ratio increase from zero. As shown in Fig. 2, the first and second gaps appear between TM0 and TM1 and between TM1 and TM2 bands, respectively, while TE modes do not have cutoff frequency and their first gap appears between first and second (TE1-2) bands. As a result, by increasing r/a ratio with fixed background dielectric constant (air background), unlike the photonic dielectric crystals, the width of bandgaps increase and the bands become more flatter for TM modes due to decreasing the group velocity. Also, the cutoff frequency of TM modes goes to larger frequencies and distance between the bands increase. Fur-

thermore, by increasing r/a ratio for TE modes, the bandgap can be observed when r/a ratio is about 0.3 and the first gap is between first and second bands. Meanwhile, the second gap appears between third and fourth bands, as illustrated in Fig. 2(b).

B. In this part, we indicate the effect of varying the noble metals used for rods on the photonic bandgaps. The photonic band structures calculate for three noble metals (Cu, Ag, and Au) with fixed r/a ratio and with air or InP background, as shown in Figs. 3 and 4. Details of results are tabulated in Table. 2. Comparing Fig. 2 with Figs. 3 and 4 shows that there is no any considerable difference in widths of the photonic band gaps of TM modes and so there is no bandgap for TE modes. Hence, one can deduce that the kind of metal rods has not substantial effect on the photonic bandgap.

C. Finally, we investigate the effect of different dielectric background on widths of the photonic band gaps for copper rods. Our simulation results are sum-

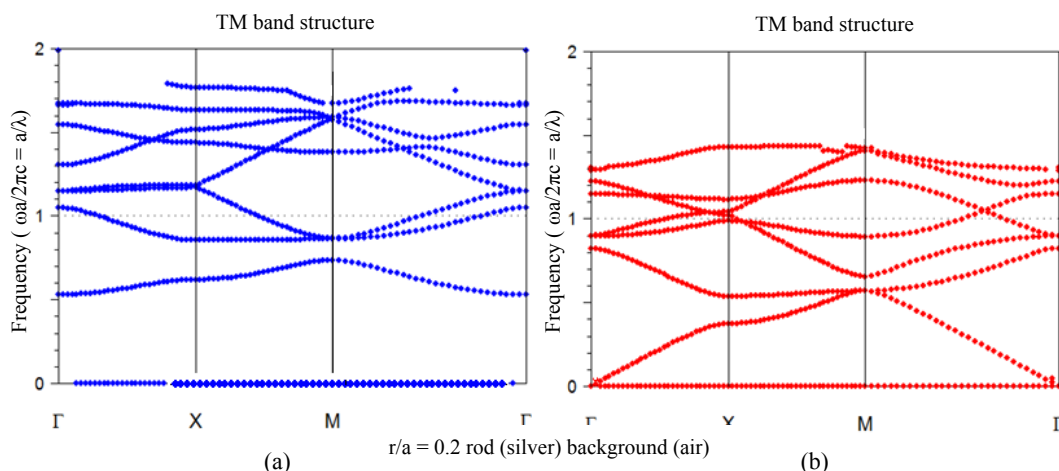


Fig. 3. Photonic band diagrams for silver rods in air background. The first 8 bands for TM (a) and TE (b) modes.

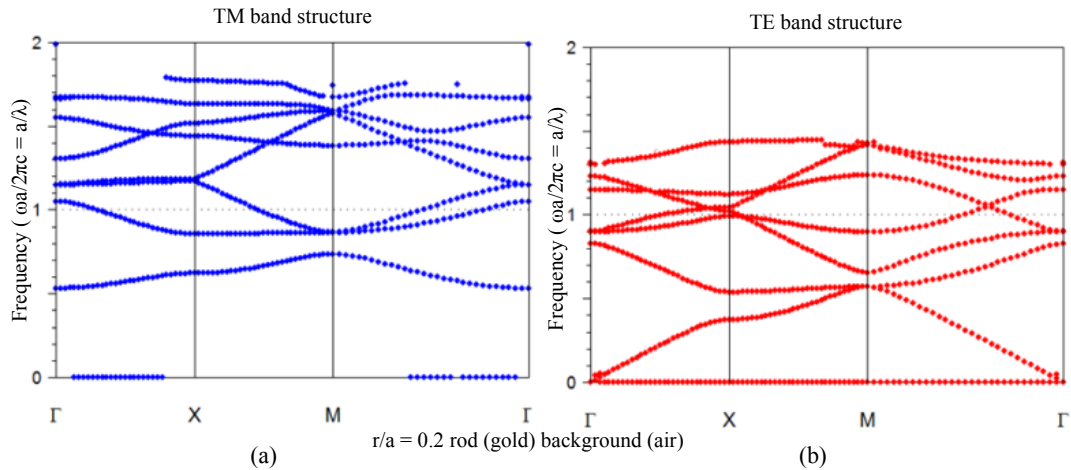


Fig. 4. Photonic band diagrams for gold rods in air background. The first 8 bands for TM (a) and TE (b) modes.

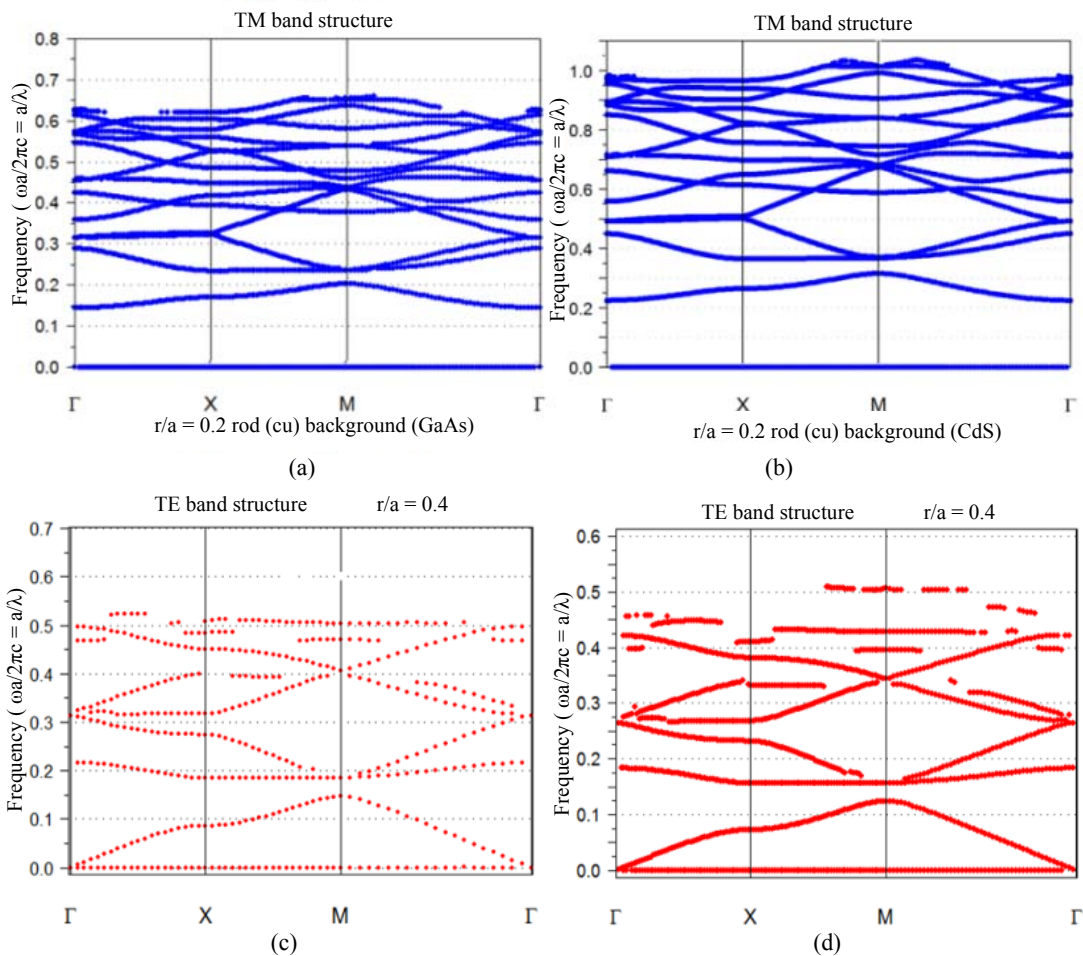


Fig.5. Band gaps diagrams for square lattice with different background. (a) GaAs and (b) CdS background for TM mode. (c) background with $\epsilon_r=8.9$ and (d) background with $\epsilon_r=12.4$ for TE mode

marized in Table 3. As shown in Fig. 5, the cutoff frequency and width of the first and second band gaps decrease by increasing dielectric constant with fixed r/a ratio.

4. Conclusions

In this paper, we have numerically analysed the photonic band structure of 2-D metallic-dielectric photonic crystal structures which consist of square arrays with circular metal rods for normal incident wave. Using the Drude model for the noble metals (Cu, Ag,

and Au), we have calculated the photonic band diagrams for TM and TE modes. The results show that TM modes have a cutoff frequency and their bandgaps appear as soon as r/a ratio increase from zero, while TE modes do not have cutoff frequency. Its cutoff frequency goes to large frequencies and distance between its bands increase. By increasing r/a , width of bandgaps increased in contrast with photonic dielectric crystals that closed. For TE mode the first gap appears when r/a starts at 0.3. Also, we studied photonic band gaps for constant r/a (0.2) for different noble metals in air/InP background. With these conditions we did not see any considerable difference between widths of gaps for different metals. Then by making r/a and metal constant, changed the dielectric constant of background. The results showed that by increasing the dielectric constant of background cutoff frequency goes to small frequencies and the width of first and second band gaps goes to small quantity. Bands become closer and go to smaller frequencies. Finally, the results showed that MDPCs can be used for various applications in optical communication such as optical add/drop filters, because those can have photonic bandgaps in wavelengths of optical communications.

Acknowledgments

The authors would like to thank Education and Research Institute for ICT (formerly, Iran Telecommunication Research Center) for the financial support of this project.

References

- [1] M. M. Sigalas, C. T. Chan, K. M. Ho, C. M. Soukoulis, *Phys. Rev. B* **52**, 11744 (1995).
- [2] A. Moroz, *Phys. Rev. Lett.* **83**, 5274 (1999).
- [3] V. Kuzmiak, A. A. Maradudin, F. Pinsemin, *Phys. Rev. B* **50**, 16835 (1994).
- [4] K. Sakoda, *Phys. Rev. B* **64**, 045116 (2001).
- [5] O. Takayama, M. Cada, *Appl. Phys. Lett.* **85**, 1311 (2004).
- [6] X. Zhang, Z.-Q. Zhang, *Phys. Rev. B* **61**, 9847 (2000).
- [7] A. Moroz, *Phys. Rev. B* **66**, 115109 (2002).
- [8] E. R. Brown, O. B. McMahon, *Appl. Phys. Lett.* **67**, 2138 (1995).
- [9] C. Jin, B. Cheng, B. Man, D. Zhang, S. Ban, B. Sun, L. Li, X. Zhang, Z. Zhang, *Appl. Phys. Lett.* **75**, 1201 (1999).
- [10] M. M. Sigalas, R. Biswas, K. M. Ho, C. M. Soukoulis, D. D. Crouch, *Phys. Rev. B* **60**, 4426 (1999).
- [11] T. D. Drysdale, *J. Vac. Sci. Technol. B* **21**, 2878 (2003).
- [12] E. Moreno, D. Erni, C. Hafner, *Phys. Rev. B* **65**, 155120 (2002).
- [13] J. D. Joannopoulos, S. G. Johnson, "Photonic Crystal Molding the Flow of Light", Second Edition, (2008).
- [14] K. Sakoda, "Optical properties of photonic crystals", Springer Verlag, Berlin, (2004).